Journal of Materials Chemistry A

Accepted Manuscript

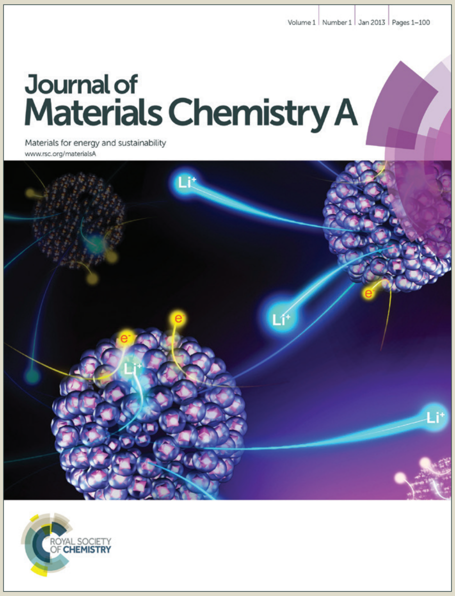

ROYAL SOCIETY OF CHEMISTRY

www.rsc.org/materialsA

Graphene-Co_3O_4 Nanocomposite as an Efficient Bifunctional Catalyst for Lithium-air Batteries

Chunwen Sun,[1*] Fan Li,[4] Chao Ma,[2] Yan Wang,[4] Yulan Ren,[3] Wei Yang,[1] Zhaohui Ma,[1] Jianqi Li,[2] Yujin Chen,[3*] Youngsik Kim,[5]* and Liquan Chen[1]

[1]Key Laboratory for Renewable Energy, Beijing Key Laboratory for New Energy Materials and Devices, Beijing National Laboratory for Condensed Matter Physics, Institute of Physics, Chinese Academy of Sciences, Beijing 100190, China

[2]Laboratory for Advanced Materials & Electron Microscopy, Beijing National Laboratory for Condensed Matter Physics, Institute of Physics, Chinese Academy of Sciences, Beijing 100190, China

[3]College of Science, Harbin Engineering University, Harbin, Heilongjiang, 150001, China

[4]College of Environmental and Energy Engineering, Beijing University of Technology, Beijing 100124, China

[5]Interdisciplinary School of Green Energy, Ulsan National Institute of Science and Technology, Ulsan (UNIST), Ulsan, Korea

[*] Corresponding authors.

Tel: +86-10-82649901, Fax: +86-10-82649046, Email: csun@iphy.ac.cn, (C. Sun)
Tel: +86-451-82519754, Fax: +86-451-82519754, Email:chenyujin@hrbeu.edu.cn (Y. Chen)
Tel : +82-52-217-2921, Fax : +82-52-217-3009, Email : ykim@unist.ac.kr, (Y. Kim)

Abstract

A facile hydrothermal route has been developed to prepare graphene-Co_3O_4 nanocomposite. The graphene-Co_3O_4 nanocomposite catalyst demonstrates an excellent catalytic activity toward oxygen reduction reaction including a much more positive half-wave potential (-0.23V) than the pristine graphene (-0.39V) as well as higher cathodic currents. Importantly, this catalyst shows a better long-term durability than the commercial Pt/C catalyst in an alkaline solution. The preliminary results indicate that the graphene-Co_3O_4 nanocomposite is an efficient and stable bifunctional catalyst for a Li-air battery. It may be as an alternative to the high-cost commercial Pt/C catalyst for the ORR/OER in alkaline solutions.

Keywords: Graphene, Co_3O_4, nanocomposite, oxygen-reduction reaction, synergistic effects

1. Introduction

The oxygen reduction reaction (ORR) is an important process in the energy conversion and storage, such as, fuel cells[1,2] and metal-air batteries[3,4]. For proton exchange membrane (PEM) fuel cells, high cost of Pt cathode and its poor durability are still main obstacles that hinder its commercial development. Among various metal-air batteries, lithium (Li)-air batteries possess the highest theoretical gravimetric energy density (11 140 Wh kg^{-1}) if oxygen is accessed directly from the air.[5] However, for the rechargeable Li-air battery, besides the challenges of cost, another issue that has to be addressed in the current technology is the limitations of ORR during discharging process and oxygen evolution reaction (OER) during charging process. The sluggish kinetics of the ORR and OER in Li-air batteries is ascribed to the low efficiency of catalysts.[4,5] The performance of the Li-air batteries can be drastically improved by incorporating an efficient catalyst to achieve higher discharge voltage, lower charge voltage and rate performance.[6] Therefore, the design of a low-cost and stable bifunctional electrocatalyst is a major challenge to the construction of efficient Li-air batteries.

The cathode catalysts normally used to catalyze the air reactions are carbon black or carbon loaded with a noble metal.[3] Oxidation of a carbon support in Li-air batteries should be paid more attention as that in the PEM fuel cell. Many spinel cobaltite oxides have been investigated as electrocatalysts for the ORR or OER.[7,8] Bruce *et al.* reported a screening of many catalysts that could be used in facilitating the electrochemical properties of the O_2 electrode in a non-aqueous Li-O_2 cell.[9] Among the various oxide catalysts studied, Co_3O_4 gives the best compromise between initial capacity and capacity retention as well as the lowest charging voltage of 4V. Recently, we demonstrated the perovskite $Sr_{0.95}Ce_{0.05}CoO_{3-\delta}$ loaded with copper nanoparticles on their surface are shown to be excellent, low-cost, and stable bifunctional catalysts for oxygen-reduction and oxygen-evolution reactions in an aqueous solution.[3] Dai *et al.* reported a hybrid material consisting of Co_3O_4 nanocrystals grown on reduced graphene oxide as a high-performance bi-functional catalyst for the ORR and OER.[10] Yang et al. demonstrated the influence of morphology on the bifunctionality of porous

Co_3O_4 microspheres for the Li-air batteries.[4] Among carbon materials, graphene, a two-dimensional aromatic monolayer of sp^2-hybridized carbon atoms, has become a promising candidate for the ORR catalysis due to its high conductivity and excellent mechanical properties, which are greatly favorable for the harsh ORR process.[11,12] Recently, the bifunctional composite catalysts of Co_3O_4 nanofibers immobilized on nonoxidized graphene nanoflakes have been demonstrated in Li-O_2 batteries by Ryu *et al.*.[13] The mechanism of Co_3O_4/graphene catalytic activity in Li-O_2 batteries with carbonate based electrolytes has been studied by Lim *et al.*.[14] To our knowledge, there are no reports on the systematic studies on ORR and OER properties of graphene (G)-Co_3O_4 nanocomposite as well as its applications as a bifunctional catalyst for Li-air batteries so far. Herein, we report highly active and stable graphene (G)-Co_3O_4 nanocomposite electrocatalysts synthesized via a facile hydrothermal route and subsequent thermal treatment process. The catalytic properties toward ORR and OER were investigated by means of cyclic voltammetry (CV) and linear sweep voltammograms (LSVs). As a bifunctional catalyst, a round-trip electric-energy storage efficiency of 76.5% for the graphene-Co_3O_4 catalysts was observed in an aqueous Li-air cell.

2. Experimental

Materials synthesis. Graphene sheets used in this work were purchased from Nanjing XFNano Material Tech Co., Ltd, and their diameter and thickness are in the range of 0.5-2 μm and 0.8 nm, respectively. The oxygen content in the greaphene is about 7wt%. The synthesized processes of graphene is described below. Typically, graphite oxide (GO) was prepared from natural graphite through a modified Hummers method.[15] The GO was thermally treated at a high temperature under N_2 flow, and then was reduced at 1200 ^oC under H_2 atmosphere.[16] To prepare graphene-cobalt oxide/cobalt composites, a hydrothermal method was used as reported previously.[17] In a typical synthesis, 0.2g of $Co(NO_3)_2.6H_2O$ was dissolved in 7ml of distilled water under magnetic stirring. 0.005 g of graphene was dispersed in the solution under ultrasonic conditions. Then 28 ml of 28-30% concentrated ammonia was slowly added. After sonication for 10 min, the mixture was transferred into a Teflon-lined stainless steel autoclave with a capacity of 50 ml for hydrothermal treatment at 100°C for 8h. As the autoclave cooled to room temperature naturally, the precipitates were separated by centrifugation, washed with distilled water and absolute ethanol, then dried under vacuum. Thus, graphene-Co_3O_4 nanocomposite was obtained by annealing at 150 °C for 30 min under Ar gas flow. After annealing at 270°C for 1 h under Ar/H_2 (10vol%) gas flow, graphene-Co nanocomposite was obtained.

Characterizations. XRD analyses were performed on a X'Pert Pro diffractometer with Cu Kα radiation (λ=1.54Å). Scanning electron microscopy (SEM) was performed on a scanning electron microscope (JEOL-JSM-6700F). High resolution scanning transmission electron microscopy (STEM) and electron energy loss spectroscopy (EELS) measurements were carried out on FEI Tecnai-F20 TEM operated at 200 kV.

Electrochemical measurements. A saturated calomel electrode (SCE) was used as the reference electrode in all measurements. Cyclic voltammetry (CV) and linear sweep voltammograms (LSVs) were conducted in a three-electrode electrochemical cell with a Pt plate (10×10×0.3 mm) and a glassy carbon (GC, ϕ =5 mm) electrode as the counter electrode and the working electrode, respectively. The Pt/C (Hispec 3000, Alfa Aesar-A Johnson Matthey Company), cobalt(II,III) oxide (Co_3O_4, Strem Chemicals, Inc.), the pristine graphene, graphene-Co and graphene-Co_3O_4 catalysts were dispersed into 1.0 mg mL^{-1} suspension with 0.05 wt% ethanol mixed with Nafion solution, respectively. Then 10 μl or 20 μl of the above suspensions were transferred onto the polished GC electrode substrates, respectively. The prepared electrodes were solidified for 0.5 hours at ambient before testing. Electrochemical measurements were performed by CV with VMP3 (Bio-Logic SA) and rotating disk electrode (RDE, M636, Pine Research Instrumentation). The scan rates were 100 mV s^{-1} for CV and 10 mV s^{-1} for ORR and OER measurements, respectively. All the potentials in LSV and CV measurements are relative to SCE.

The aqueous Li-air battery was assembled as that previously described.[3] The air catalytic electrode included a catalyst layer and a gas-diffusion layer. Teflon-treated carbon paper (Fuel Cell Store, Inc., 200 μm in thickness) was used as the gas diffusion layer. Catalyst ink solutions were prepared by mixing the catalyst (80 wt.%) with ionomer (Tokuyama A4, 20wt.%) as a binder and tetrahydrofuran (Acros Organics) as a solvent in an ultrasonic bath for 1 h. The ink solution was sprayed onto one side of the Teflon-treated carbon paper. The area of the air electrode was 4 cm^2, and the mass loading of the catalyst sample was ~1.25 mg with a thickness of approximately 10 μm. The assembled Li-air battery was exposed to ambient air and connected to the testing station. A Solartron 1470 cell tester was employed to perform the charge and discharge tests at different current densities.

3. Results and Discussion

The crystallinity and purity of the as-synthesized samples were investigated by X-ray powder diffraction (XRD). Fig. 1a shows a typical XRD pattern of the graphene-Co_3O_4 nanocomposite prepared under Ar atmosphere. In the XRD pattern, all diffraction peaks can be indexed to a cubic phase Co_3O_4 (JCPDS 43-1003). An additional small and broad diffraction peak that appears at 2θ of 22.5-27.5^o can be indexed to the disordered graphene sheets. It indicates that the composite consists of the well-crystallized Co_3O_4 and the disorderedly stacked graphene sheets. After the graphene-Co_3O_4 composite is annealed at 270^{o}C for 1 h under Ar/H_2 gas flow, the graphene-Co nanocomposite is obtained. Fig. 1b shows a typical XRD pattern that consists of the mixture of hexagonal phase cobalt (JCPDS 05-0727) and face-centered cubic phase cobalt (JCPDS 89-4307). It implies that the Co_3O_4 in the composite is transformed into the metallic cobalt after the thermal treatment in Ar/H_2 gas flow. In addition, a weak diffraction hump at 2θ of 20-30 assigned to the graphene is still present in the pattern, suggesting that the nanocomposite consists of graphene and cobalt.

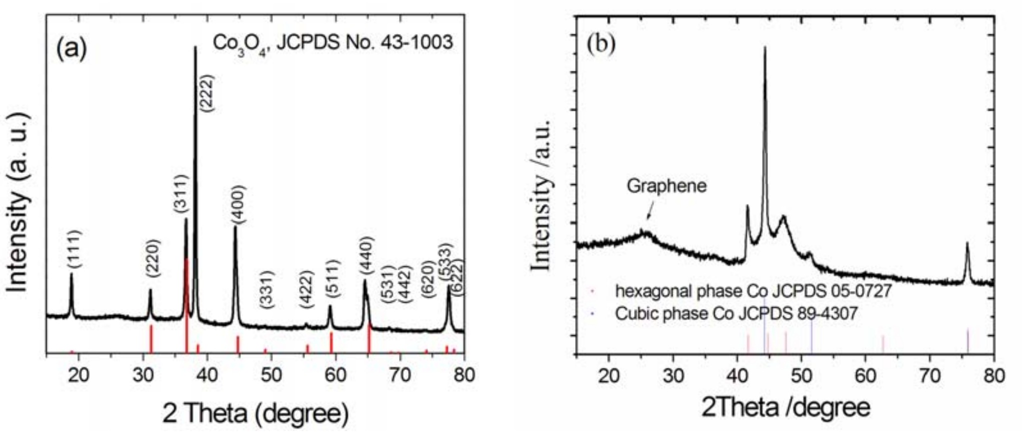

Fig. 1 XRD patterns of (a) the product synthesized under Ar atmosphere and (b) the product synthesized under H_2-Ar atmosphere.

The size and morphology of the products were examined by SEM and TEM measurements. Low-magnification SEM and TEM images show that Co_3O_4 and Co nanoparticles are well dispersed on the surface of the graphene sheets. Fig. 2b and 3b show annular dark-field (ADF) scanning transmission electron microscopy (STEM) images of the as-prepared graphene-Co_3O_4 prepared under Ar and H_2-Ar atmosphere, respectively. It displays that the Co_3O_4 particles have a diameter of about 200 nm and consist of many smaller NPs, forming a porous structure as shown in Fig. 2c. However, the Co nanoparticles have a similar size but with a solid structure (Fig. 3c). It indicates that the calcination atmosphere plays an import role in the morphology of the resultant products. Both the excellent conductivity property of the graphene and the excellent catalytic properties of Co_3O_4 as well as its porous characteristic are expected to have favorable functions for ORR and OER.[18-21]

To further clarify the chemical composition of the samples obtained under different atmosphere, the electron energy loss spectroscopy (EELS) analysis is also shown in Fig. 2d and 3d. It reveals the characteristic Co and O-shell ionization edges. These results further clearly indicate that nanoparticles on the graphene prepared under Ar and H_2-Ar atmosphere are Co_3O_4 and Co, respectively.

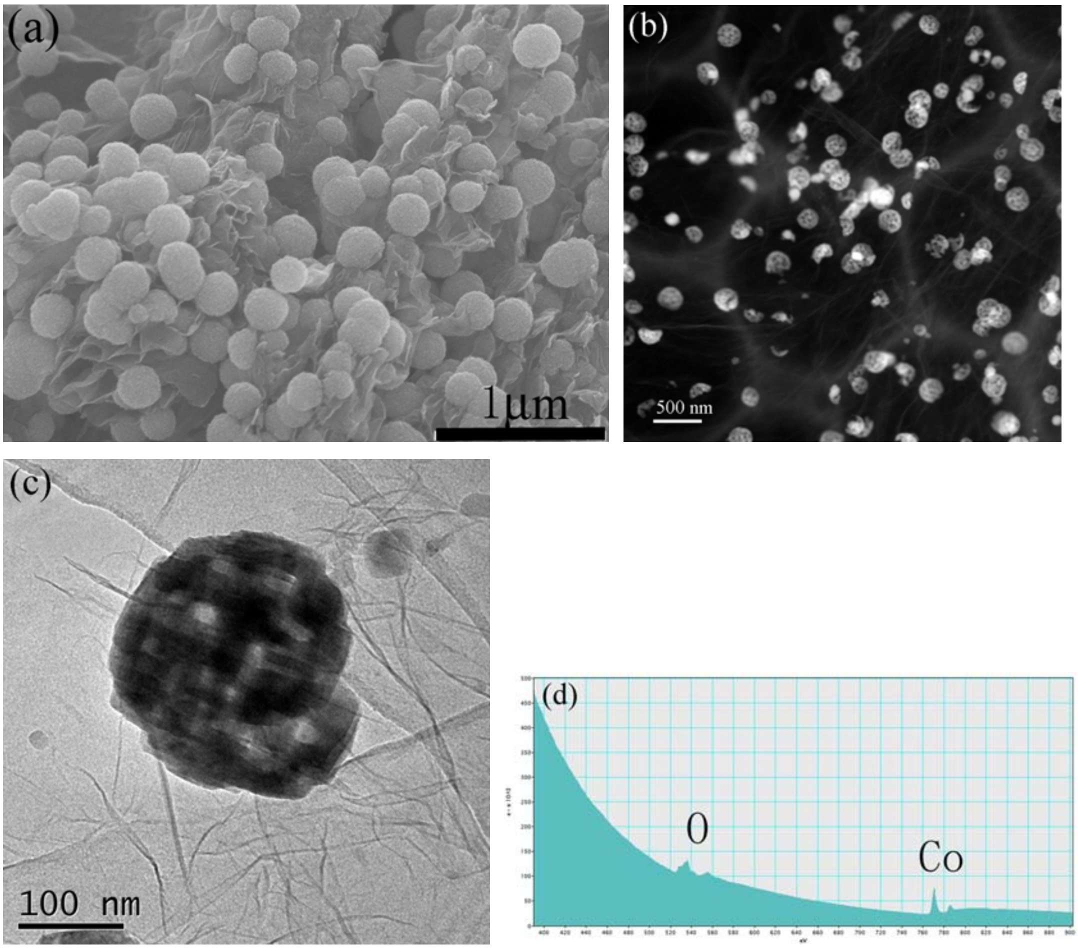

Fig. 2 (a) SEM, (b) ADF-STEM, and (c) TEM images of the as-prepared graphene-Co_3O_4 prepared under Ar atmosphere, (d) The corresponding EELS analysis taken at the nanoparticle.

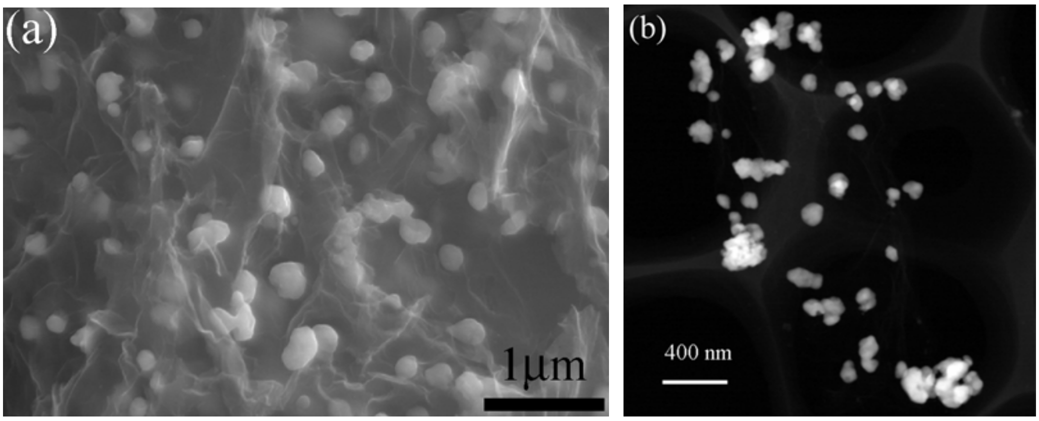

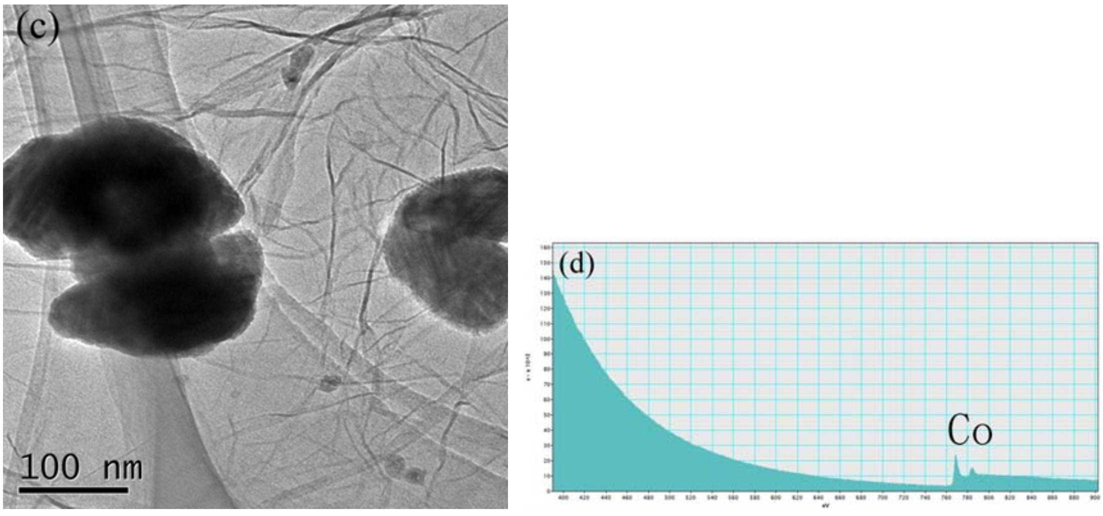

Fig. 3 (a) SEM, (b) ADF-STEM, and (c) TEM images of the as-prepared graphene-Co prepared under H_2-Ar atmosphere, (d) The corresponding EELS analysis taken at the nanoparticle.

The ORR catalytic activities of the graphene-Co_3O_4 composites prepared under different atmosphere were studied by the rotating disk electrode (RDE) in the O_2-saturated 0.1M KOH solution and compared with those of the commercial Pt/C, commercial Co_3O_4 and the pristine graphene catalysts. Fig. 4a shows the cyclic voltammetry (CV) curves of the pristine graphene, commercial Co_3O_4 and the graphene-Co_3O_4 composite in O_2 or Ar-saturated 0.1 M KOH solution. There are apparent cathodic peak in O_2-saturated 0.1 M KOH solution, which are ascribed to the electrocatalytic oxygen reduction on the electrode. For fuel cells and metal air batteries, an oxygen cathode with a high working potential leads to sufficiently high energy conversion efficiency. Therefore, it is important to compare the potential of oxygen reduction for different catalysts.[22,23] A better catalyst is characterized by a higher induced current density at a given applied potential or a more positive ORR onset potential. As shown in Fig. 4a, the graphene-Co_3O_4 composite shows a much positive ORR peak potential (~ -0.23V) than the pristine graphene and shows higher cathodic currents. Fig. 4b clearly shows the onset potential of the graphene-Co_3O_4 composite (~ -0.11 V), which is higher than the pristine graphene (~ -0.21 V) and the commercial Co_3O_4 (~ -0.31 V). Alternatively, the half-wave potential, a potential at which the current is a half of the limiting current in a LSV curve, has also been widely used for this purpose.[18] As can be seen from Fig. 4b, the current density of the graphene-Co_3O_4 composite at the half-wave potential is 2.34 mA cm^{-2}, which is about 2.41 and 2.21 times of that of the commercial Co_3O_4 (0.97 mA cm^{-2}) and the pristine graphene (1.06 mA cm^{-2}), respectively. Fig. S1b shows the ORR polarization curves obtained at a rotation rate of 1600 rpm. Both the positive potential and higher current density suggests there is a synergetic effect in the Co_3O_4-graphene catalysis for the ORR.

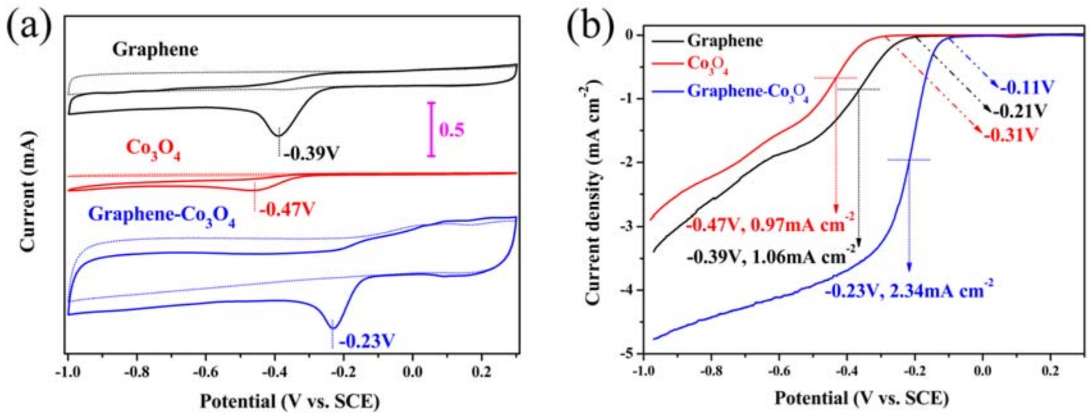

Fig. 4 Electrochemical ORR catalytic performance on different catalysts: (a) CV curves of the Co_3O_4-graphene composite, the commercial Co_3O_4 and the pristine graphene on glassy carbon electrodes in O_2-saturated (solid line) or Ar-saturated 0.1M KOH (dash line) with a scan rate of 100 mV s^{-1}, (b) ORR polarization curves of different catalysts at a scan rate of 10 mV s^{-1} and a rotation speed of 1600 rpm in O_2-saturated 0.1M KOH solution. Catalyst loading was 0.102 mg cm^{-2} for all catalysts.

To gain more insight into the ORR process on the various catalysts, linear sweep voltammograms on a RDE were recorded at different rotating speeds from 400 rpm to 3600 rpm in 0.1M KOH electrolyte saturated with O_2. It can be seen that the limiting current density increases with increasing rotation rate (Fig. 5a and 5c). The corresponding Koutecky-Levich (K-L) plots (Fig. 5b and 5d) show the inverse current

(i^{-1}) as a function of the inverse of the square root of the rotation speed ($\omega^{-1/2}$) at different potential values. For comparison, Fig. S2b shows the K-L plots of the commercial Pt/C catalyst. The linearity of the K-L plots and near parallelism of the fitting lines at different potentials from -0.4V to -0.9V suggests first-order reaction kinetics toward the concentration of dissolved O_2 on various catalysts.[10] The number of electrons involved per O_2 in the ORR on various catalysts was determined by the Koutecky-Levich equation:[10]

$$\frac{1}{j} = \frac{1}{j_k} + \frac{1}{B\omega^{1/2}} \qquad (1)$$

where j_k is the kinetic current and ω is the angular velocity, and B is determined from the slope of the K-L plots based on the Levich equation as follows.

$$B=0.62nFC_{O_2}(D_{O_2})^{2/3}\nu^{-1/6} \qquad (2)$$

where n represents the number of electrons transferred per oxygen molecule (O_2), F is the Faraday constant (96485 C mol^{-1}), D_{O_2} is the diffusion coefficient of O_2 in 0.1M KOH (1.9×10^{-5} $cm^2\,s^{-1}$), ν is the kinetic viscosity (0.01 $cm^2\,s^{-1}$), and C_{O_2} is the bulk concentration of O_2 (1.2×10^{-6} mol cm^{-3}).[12] The electron transfer number (n) in Equation (2) for the commercial Pt/C, graphene-Co_3O_4, and graphene-Co can be determined from the slopes of the K-L plots at -0.6V to be about 4, 3.47 and 3.64, respectively. The calculated electron transfer numbers for the graphene-Co_3O_4, and graphene-Co are comparable to those graphene based catalysts.[12,23,24] It indicates the ORR on the graphene-Co_3O_4/Co catalysts favor a four electrons process.

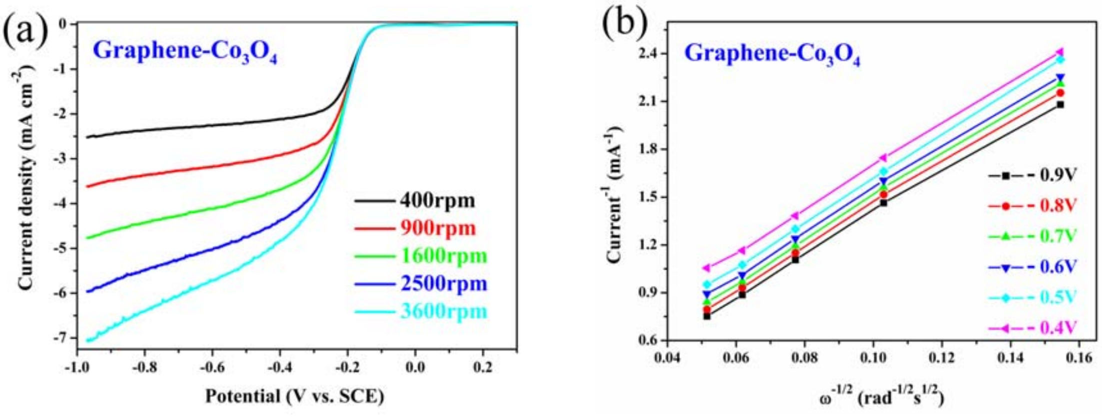

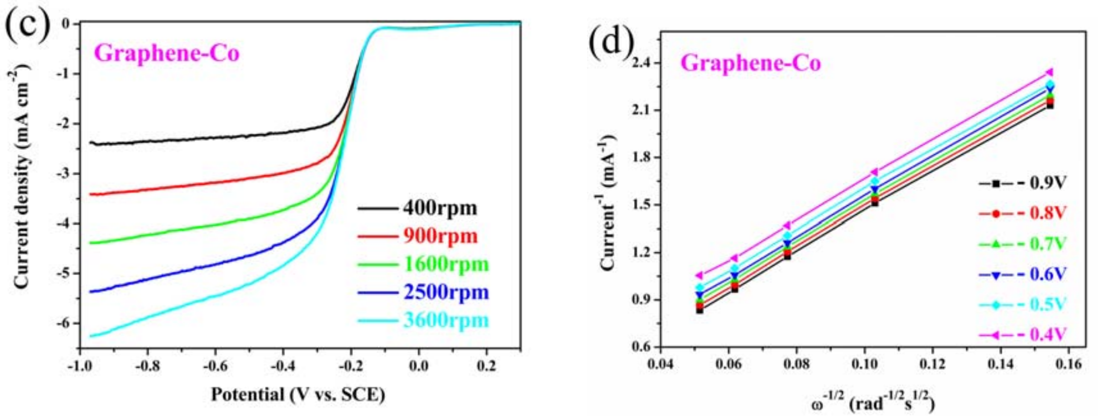

Fig. 5 LSVs at different rotating speeds and K-L plots of different catalysts at various potentials tested in O_2-saturated 0.1M KOH: (a,b) the graphene-Co_3O_4 catalyst, (c,d) the graphene-Co catalyst.

Long-term stability of catalysts is an important parameter for their applications. To examine and compare the durability of the Pt/C and graphene-Co_3O_4/Co prepared under different atmosphere, cyclic voltammetries were performed at a scan rate of 100 mV s^{-1} under ambient condition. As shown in Fig. 6a, the solid lines and dash lines correspond to the 1st and the 3000th scanning, respectively. After the 1st and the 3000th CV scanning, the LSV curves of different catalysts were also recorded at a scan rate of 10 mV s^{-1} and a rotation speed of 1600 rpm in O_2-saturated 0.1M KOH solution, shown in Fig. 6b, 6c, 6d, respectively. It can be seen clearly that the current densities were decreased with the scanning time increasing. Thus, the degradation rate was calculated by the following Equation.

$$\text{Loss of current density } \% = (j_{1\mathrm{st}} - j_{3000\mathrm{th}}) / j_{1\mathrm{st}} \qquad (3)$$

where $j_{1\mathrm{st}}$ and $j_{3000\mathrm{th}}$ are the current density in the 1st and the 3000th LSV scanning at -0.2 V, respectively. The losses of current densities of the Pt/C, graphene-Co_3O_4, graphene-Co catalysts were determined to be 48.8%, 46.5% and 50.6%, respectively. Therefore, the graphene-Co_3O_4 shows a better long-term stability than the Pt/C catalyst in alkaline solution. It is usually believed that the electrochemical corrosion of the carbon support is one of the most critical issues that affect the durability of the Pt/C catalyst.[25-30] These results indicate that graphene-based composites have better corrosion-resistant performance in alkaline solution.

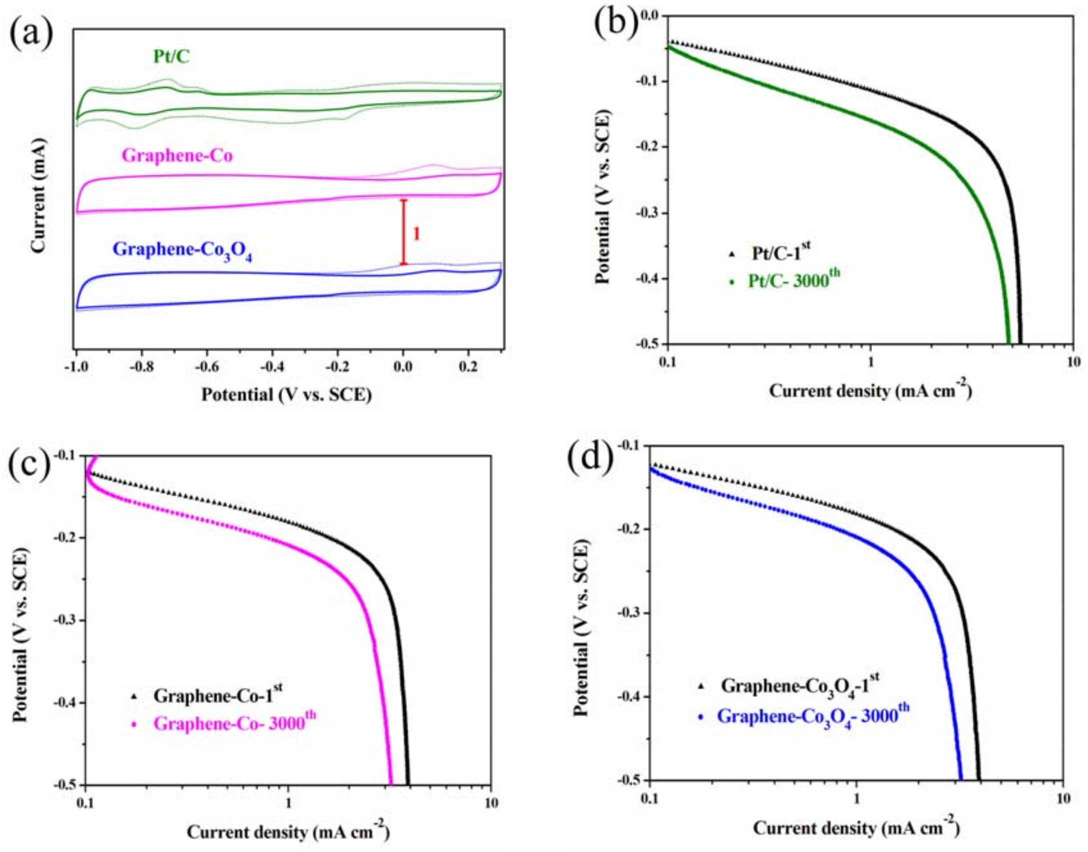

Fig. 6 Comparison of the long-term stability of the Pt/C, graphene-Co_3O_4 and graphene-Co prepared under different atmosphere: (a) cyclic voltammetries were scanned at a scan rate of 100 mV s^{-1} under ambient condition; (b-d) LSV curves of different catalysts recorded at a scan rate of 10 mV s^{-1} and a rotation speed of 1600 rpm in O_2-saturated 0.1M KOH solution.

To study the electrocatalytic activity of the catalysts for OER, LSV was performed with the pristine graphene, the commercial Co_3O_4 and the graphene-Co_3O_4 loaded on the glassy carbon electrodes measured in an Ar-saturated 0.1 M KOH solution with a scan rate of 10 mV s^{-1}. As shown in Fig. 7a, the graphene-Co_3O_4, the pristine graphene, the commercial Co_3O_4 catalysts result in a current density of 1.5 mA cm^{-2} at a potential of 0.65 V, 0.69 V and 0.73V, respectively. Tafel plots of LSVs are derived and shown in Fig. 7b, from which small Tafel slopes down to 67.8, 69.1 and 71.4 mV per decade were found for the graphene-Co_3O_4, the pristine graphene, the commercial Co_3O_4 catalysts, respectively. Similar to that of ORR, the graphene-Co_3O_4 also shows a synergetic effect for OER considering a decreased overpotential and a smaller Tafel slope.

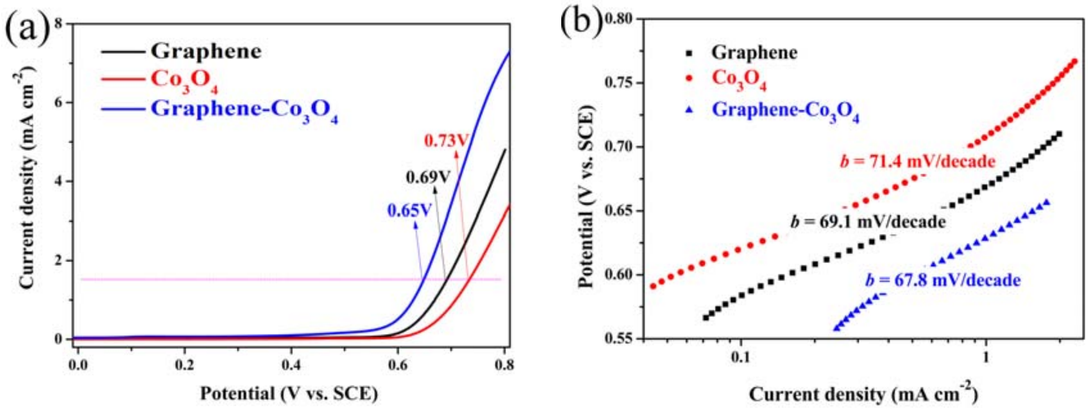

Fig. 7 (a) Oxygen evolution currents of the pristine graphene, the commercial Co_3O_4 and the graphene-Co_3O_4 on glassy carbon electrodes measured in an Ar-saturated 0.1 M KOH solution with a scan rate of 10 mV s^{-1}. (b) Tafel plots of OER currents in Fig. (a). Catalyst loading was 0.051 mg cm^{-2} for all the three catalysts.

For a rechargeable Li-air battery, a bifunctional electrocatalyst is required for simultaneously catalyzing ORR and OER reactions. In this work, we further examine the potential application of the graphene-Co_3O_4 catalyst in the rechargeable Li-air battery. The catalyst was tested in a cell with hybrid electrolytes as previously described in the reference.[3] The first discharge and charge curves of the cell with the graphene-Co_3O_4 catalyst were compared with those tested with Vulcan XC-72 and state-of-the-art 50% Pt/carbon-black catalyst, as shown in Fig. 8a. The discharge voltage of the cells with the graphene-Co_3O_4 catalyst is lower than that of the 50% Pt/carbon-black catalyst, but higher than that of the Vulcan XC-72 at the rate of 80 mA g^{-1}. It is obvious that the charge voltage of cells with the graphene-Co_3O_4 catalyst is lower than that of the Vulcan XC-72. It means that the graphene-Co_3O_4 catalyst is more effective for OER.

The difference between discharge and charge voltages (ΔV) as marked in Fig. 8a for the Vulcan XC-72, the commercial Co_3O_4 powder, the graphene-Co_3O_4 and 50%Pt/C catalysts are 1.43V, 1.65 V, 0.97V and 0.68V, respectively, at the current rate of 80 mA g^{-1}. The round-trip efficiency (the ratio of discharge to charge voltage) is 76.5% for the cell with the graphene-Co_3O_4 catalyst. This value is lower than that of the 50% Pt/C catalyst (83.0%), but higher than those of the Vulcan XC-72 (67.6%) and the commercial Co_3O_4 powder (63.8%). The discharge voltage of the commercial Co_3O_4 powder in micro meter size (Aldrich) is lower than that of the graphene-Co_3O_4, and the charge voltage is much higher (Fig. 8a). In addition, the graphene-Co_3O_4 is also operated well at high current rates (Fig. 8b). Fig. 8c shows the charge/discharge curves at a current density of 160 mA g^{-1}. It clearly indicates that the cell can be reversibly charged/discharged and the graphene-Co_3O_4 catalyst has a good cycle performance. It was reported in recent literatures that Li-O_2 batteries tested with pure oxygen exhibited an improved cycle performance with a larger capacity.[31] However, the electrochemical performances of the cell was sharply degraded when tested under air atmosphere due to complex reactions arising from CO_2 and H_2O in air as well as the clog effect of the discharged product Li_2O_2 in the porous electrode. In contrast to Li-O_2 batteries, our cell was exposed to air atmosphere during cycling of the cell, which was designed to test real air as the cathode for Li-air battery. Although the recent Li-O_2 batteries with non-aqueous electrolyte showed a relatively large capacity at the first cycle, they quickly degradaded with cycling even tested under pure oxygen atmosphere.[32-34] It is worth pointing out that there is a limitation arising from the solid electrolyte plate used for cell testing. The commercial solid electrolyte that is commonly used in an aqueous Li-air battery is $Li_{1+x+y}Al_xTi_{2-x}Si_yP_{3-y}O_{12}$ (OHARA Inc., Japan). This solid electrolyte has been known to be unstable in alkali liquid electrolytes for a long period time (>100 h), which will eventually affect the cell voltage and cycle life.[35-37] Thus, the cycle test in this work was performed with a limited discharge-charge depth of 200 mAh/g and at the current rate of 160 mA/g. Considering the higher round-trip efficiency and excellent long-term stability as well as lower cost compared with noble metal catalysts, the graphene-Co_3O_4 material is a promising bifunctional catalyst for the Li-air battery.

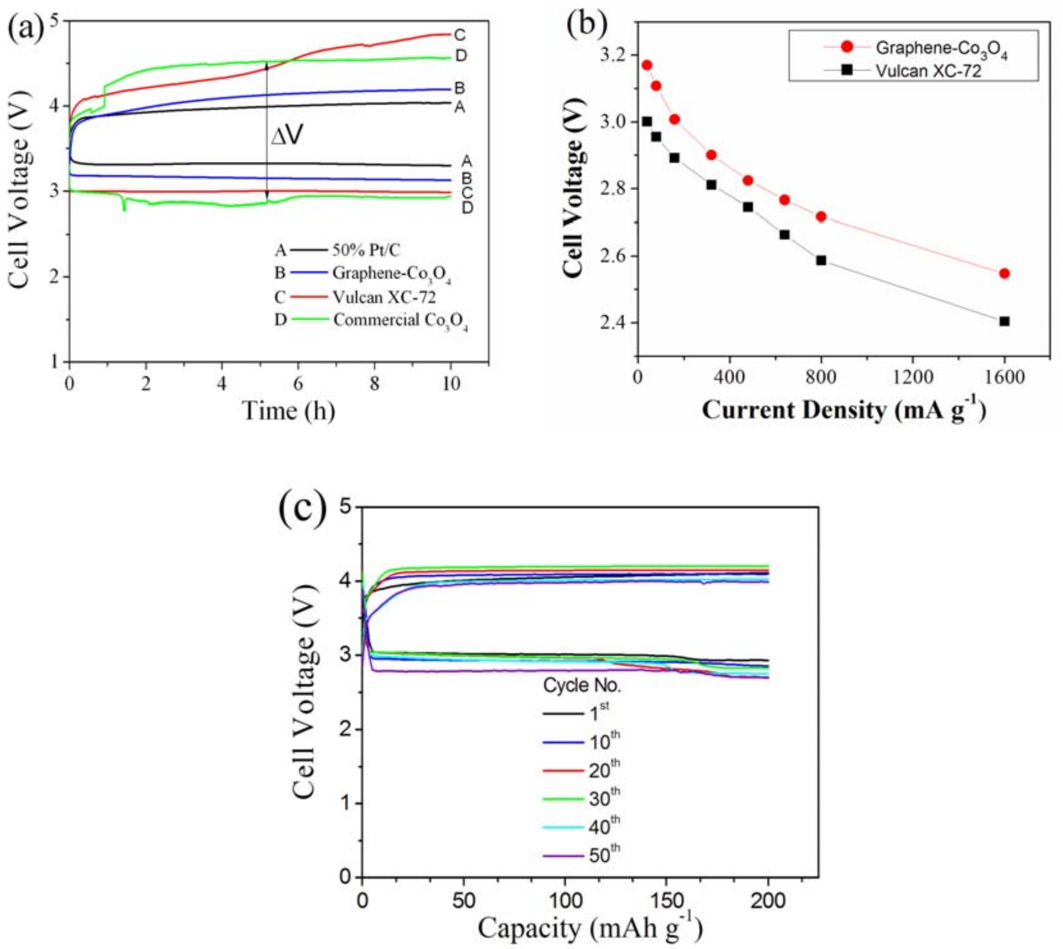

Fig. 8 (a) Comparison of the first charge and discharge curves of the prepared Li-air batteries with various catalysts at a current density of 80 mA g^{-1}, (b) comparison of discharge voltage as a function of current densities at different current densities between Vulcan XC-72 and the graphene-Co_3O_4 catalyst, (c) the discharge-charge curves of the prepared Li-air batteries with the graphene-Co_3O_4 catalyst at a current density of 160 mA g^{-1} at different cycles. Catalyst loading was 1.25 mg.

4. Conclusion

In summary, we have successfully prepared the graphene-Co_3O_4 nanocomposite via a combined hydrothermal method and subsequent thermal treatment process. The obtained graphene-Co_3O_4 nanocomposite catalyst shows efficient and stable ORR and OER catalytic activities. Importantly, this catalyst shows a better long-term durability than the commercial Pt/C catalyst in an alkaline solution. It may be as an alternative to the commercial Pt/C catalyst for the ORR/OER in alkaline solutions. The improved performance of the graphene-Co_3O_4 nanocomposite catalyst can be ascribed to the synergetic effect of Co_3O_4 and graphene. We believe that the present synthetic strategy can be extended to develop other 3D oxide/metal-graphene composites for various applications, such as batteries, supercapacitors and sensors.

ACKNOWLEDGMENT

This work is financially supported by the National Science Foundation of China (NSFC) (Grant Nos. 51372271, 51172275, 51172007, 11004229) and the Institute of Physics (IOP) start-up funding. Y. Chen's work is supported by the National Natural Science Fund of China (Grant No 51272050) and Program for New Century Excellent Talents in University (NECT-10-0049). Y. Kim's work was supported by the 2013 Research Fund (1,130064,01) of UNIST (Ulsan National Institute of Science and Technology).

AUTHOR CONTRIBUTIONS

C.W.S. conceived and designed this work; C.W.S., Y.J.C., F. L. and Y.K. designed the experiments; Y.J.C. and Y.L.R. prepared the graphene-Co_3O_4/Co samples; C.M. and J.Q.L. performed TEM characterization; Y.J.C., W.Y. and Z.H.M. carried out the SEM and XRD characterizations; F.L. and Y.W. did CV and LSV tests; Y. K. tested the Li-air batteries; all the authors participated in analysis and discussions of the results and in preparing the manuscript.

REFERENCES

[1] B. Lim, M. Jiang, P.H.C. Camargo, E.C. Cho, J. Tao, X. Lu, Y. Zhu, Y. Xia, Pd-Pt bimetallic nanodendrites with highly activity for oxygen reduction, *Science*, 2009, **324**, 1302-1305.

[2] C. Sun, R. Hui, J. Roller, Cathode materials for solid oxide fuel cells: A review, *J. Solid State Electrochem.*, 2010, **14**, 1125-1144.

[3] W. Yang, J. Salim, S. Li, C. Sun, L. Chen, J.B. Goodenough, Y. Kim, Perovskite $Sr_{0.95}Ce_{0.05}CoO_{3-\delta}$ loaded with copper nanoparticles as a bifunctional catalyst for

lithium-air batteries, *J. Mater. Chem.*, 2012, **22**, 18902-18907.

[4] W. Yang, J. Salim, C. Ma, Z. Ma, C. Sun, J. Li, L. Chen, Y. Kim, Flowerlike Co_3O_4 microspheres loaded with copper nanoparticles as an efficient bifunctional catalyst for lithium-air batteries, *Electrochem. Commun.*, 2013, **28**, 13-16.

[5] A. Christensen, P. Albertus, R.S. Sanchez-Carrera, T. Lohmann, B. Kozinsky, R. Liedtke, J. Ahmed, A. Kojic, A Critical Review of Li/Air Batteries, *J. Electrochem. Soc.*, 2012, **159**, R1-R30.

[6] Y. Lu, Z. Xu, H.A. Gasteiger, S. Chen, K. Hamad-Schifferli, S. H. Yang, Platinum-gold nanoparticles: a highly active bifunctional electrocatalyst for rechargeable lithium-air batteries, *J. Am. Chem. Soc.*, 2010, **132**, 12170-12171.

[7] M. Hamdani, R.N. Singh, P. Chartier, Co_3O_4 and Co-based spinel oxides bifunctional oxygen electrodes, *Int. J. Electrochem. Sci*, 2010, **5**, 556-577.

[8] J. Xu, P. Gao, T.S. Zhao, Non-precious Co_3O_4 nano-rod electrocatalyst for oxygen reduction in anion-exchange membrane fuel cells, *Energy Environ. Sci.*, 2012, **5**, 5333-5339.

[9] A. Débart, J. Bao, G. Armstrong, P.G. Bruce, An O_2 cathode for rechargeable lithium batteries: the effect of a catalyst, *J. Power Sources*, 2007, **174**, 1177-1182.

[10] Y. Liang, Y. Li, H. Wang, J. Zhou, J. Wang, T. Regier, H. Dai, Co_3O_4 nanocrustals on graphene as a synergistic catalyst for oxygen reduction reaction, *Nature Mater.*, 2011, **10**, 780-786.

[11] S. Yang, L. Zhi, K. Tang, X. Feng, J. Maier, K. Müllen, Efficient synthesis of heteroatom (N or S)-doped graphene based on ultrathin graphene oxide-porous silica sheets for oxygen reduction reactions, *Adv. Funct. Mater.*, 2012, **22**, 3634-3640.

[12] J. Liang, Y. Jiao, M. Jaroniec, S.Z. Qiao, Sulfur and nitrogen dual-doped mesoporous graphene electrocatalyst for oxygen reduction with synergistically enhanced performance, *Angew. Chem. Int. Ed.*, 2012, **51**, 11496-11500.

[13] W. Ryu, T. Yoon, S.H. Song, S. Jeon, Y. Park, I. Kim, Bifunctional composite catalysts using Co_3O_4 nanofibers immobilized on nonoxidized grapheme

nanoflakes for high-capacity and long-cycle Li-O_2 batteries, *Nano Lett.*, 2013, **13**, 4190-4197.

[14] H. Lim, H. Gwon, H. Kim, S. Kim, T. Yoon, J.W. Choi, S.M. Oh, K. Kang, Mechanism of Co_3O_4/grapheme catalytic activity in Li-O_2 batteries using carbonate based electrolyte, *Electrochimica Acta*, 2013, **90**, 63-70.

[15] W.S. Hummers, R.E. Offeman, Preparation of graphitic oxide, *J. Am. Chem. Soc.*, 1958, **80**, 1339.

[16] Y. Ren, C. Zhu, S. Zhang, C. Li, Y. Chen, P. Gao, P. Yang, Q. Ouyang, Three-dimensional SiO_2@Fe_3O_4 core/shell nanorod array/graphene architecture: synthesis and electromagnetic absorption properties, *Nanoscale*, 2013, **5**, 12296-12303

[17] Y. Chen, Q. Wang, C. Zhu, P. Gao, Q. Ouyang, T. Wang, Y. Ma, C. Sun, Graphene/porous cobalt nanocomposite and its noticeable electrochemical hydrogen storage ability at room temperature, *J. Mater. Chem.*, 2012, **22**, 5924–5927.

[18] L. Su, Y. Jing, Z. Zhou, Li ion battery materials with core-shell nanostructures, *Nanoscale*, 2011, **3**, 3967-3983.

[19] M. Yang, J.X. Li, H.H. Li. L.W. Su, J.P. Wei, Z. Zhou, Mesoporous slit-structured NiO for high-performance pseudocapacitors, *Phys. Chem. Chem. Phys.*, 2012, **14**, 11048-11052.

[20] S.M. Yuan, J.X. Li, L.T. Yang, L.W. Su, L. Liu, Z. Zhou, Preparation and lithium storage performances of mesoporous Fe_3O_4@C microcapsules, *ACS Appl. Mater. Interfaces*, 2011, **3**, 705-709.

[21] Z. Zhang, L. Su, M. Yang, M. Hu, J. Bao, J. Wei, Z. Zhou, A composite of Co nanoparticles highly dispersed on N-rich carbon substrates: an efficient electrocatalyst for Li-O_2 battery cathodes, *Chem. Commun*, 2014, **50**, 776-778.

[22] S. Wang, L. Zhang, Z. Xia, A. Roy, D.W. Chang, J. Baek, L. Dai, BCN graphene as efficient metal-free electrodecatalyst for the oxygen reduction reaction, *Angew. Chem. Int. Ed.*, 2012, **51**, 4209-4212.

[23] S. Guo, S. Zhang, L. Wu, S. Sun, Co/CoO nanoparticles assembled on graphene

for electrochemical reduction of oxygen, *Angew. Chem. Int. Ed.*, 2012, **51**, 11770-11773.

[24] Z. Liu, G. Zhang, X. Jin, Z. Chang, X. Sun, One-step scalable preparation of N-doped nanoporous carbon as high-performance electrocatalysts for oxygen reduction reaction, *Nano Res.*, 2013, **6**, 293-301.

[25] L.M. Roen, C.H. Paik, T.D. Jarvi, Electrocatalytic corrosion of carbon support in PEMFC cathodes, *Elctrochem. Solid-State Lett.* 2004, **7**, A19-A22.

[26] E. Antolini, Formation, microstructural characteristics and stability of carbon supported platinum catalysts for low temperature fuel cells, *J. Mater. Sci.*, 2003, **38**, 2995-3005.

[27] K.H. Kangasniemi, D.A. Condit, T.D. Jarvi, Characterization of Vulcan Electrochemically oxidized under simulated PEM fuel cell conditions, *J. Electrochem. Soc.*, 2004, **151**, E125-E132.

[28] X. Wang, W. Li, Z. Chen, M. Waje, Y. Yan, Durability investigation of carbon nanotube as catalyst support for proton exchange membrane fuel cell, *J. Power Sources*, 2006, **158**, 154-159.

[29] Y. Shao, G. Yin, Y. Gao, P. Shi, Durability Study of Pt ∕ C and Pt ∕ CNTs Catalysts under Simulated PEM Fuel Cell Conditions, *J. Electrochem. Soc.*, 2006, **153**, A1093-A1097.

[30] R. Borup, J. Meyers, B. Pivovar, Y.S. Kim, R. Mukundan, N. Garland, D. Myers, M. Wilson, F. Garzon, D. Wood, P. Zelenay, K. More, K. Stroh, T. Zawodzinski, J. Boncella, J.E. McGrath, M. Inaba, K. Miyatake, M. Hori, K. Ota, Z. Ogumi, S. Miyata, A. Nishikata, Z. Siroma, Y. Uchimoto, K. Yasuda, K.I. Kimijima, N. Iwashita, Scientific aspects of polymer electrolyte fuel cell durability and degradation. *Chem. Rev.*, 2007, **107**, 3904-3851.

[31] D. Xu, Z.L. Wang, J.J. Xu, L.L. Zhang, L.M. Wang, X.B. Zhang, A stable sulfone based electrolyte for high performance rechargeable Li–O_2 batteries *Chem. Commun.*, **2012**, *48*, 11674-11676.

[32] Y. Yu, B. Zhang, Y. He, Z. Huang, S. Oh, J. Kim, Mechanisms of capacity degradation in reduced grapheme oxide/α-MnO_2 nanorod composite cathodes of

Li-air batteries, *J. Mater. Chem. A*, 2013, **1**, 1163-1170.

[33] K. Guo, Y. Li, J. Yang, Z. Zou, X. Xue, X. Li, H. Yang, Nanosized Mn-Ru binary oxides as effective bifunctional cathode electrocatalysts for rechargeable Li-O_2 batteries, *J. Mater. Chem. A*, 2014, **2**, 1509-1514.

[34] L. Xu, J. Ma, B. Li, F. Kang, A novel air electrode design: A key to high rate capability and long life span, *J. Power Sources*, 2014, **255**, 187-196.

[35] S. Hasegawa, N. Imanishi, T. Zhang, J. Xie, A. Hirano, Y. Takeda, O. Yamamoto, Study on lithium/air secondary batteries- Stability of NASICON-type lithium ion conducting glass-ceramic with water, *J. Power Sources*, 2009, **189**, 371-377.

[36] T. Zhang, N. Imanishi, Y. Shimonishe, A. Hirano, J. Xie, Y. Takeda, O. Yamamoto, N. Sammes, Stability of a water-stable lithium metal anode for a lithium-air battery with acetic acid-water solutions, *J. Electrochem. Soc.*, 2010, **157**, A214-A218.

[37] T. Zhang, N. Imanishi, Y. Takeda, O. Yamamoto, Aqueous lithium/air rechargeable batteries, *Chem. Lett.*, 2011, **40**, 668-673.

Table of Contents (TOC)

Graphene-Co_3O_4 nanocomposite as an efficient bifunctional catalyst for lithium-air batteries